DC Magnetization of transformers

Journal:	*IEE Proc. Electric Power Applications*
Manuscript ID:	EPA-2005-0440.R1
Manuscript Type:	Research Paper
Keyword:	DC injection, transformer saturation

DC Magnetization of Transformers

A. Ahfock and A. J. Hewitt

Abstract - A high enough DC component in the current on the secondary side of a transformer causes distortion of the primary side current. Prediction of such distortion relies on the availability of magnetization curves that extend deep enough into saturation. A simple test, carried out at rated voltage, is proposed which allows the magnetization curve to be deduced from measured data. In addition, a systematic procedure has been developed to evaluate the primary current distortion in both single and three phase transformers. Comparison between theoretical predictions and practical measurements are made with reasonable agreement between the two.

Index Terms - DC injection, transformer saturation

NOMENCLATURE

v = instantaneous supply voltage
ψ = instantaneous primary side core flux linkage
$\bar{\psi}$ = DC component of ψ
$\tilde{\psi}$ = instantaneous primary side core flux linkage with $\bar{\psi}$ removed
i_t = total instantaneous primary referred magnetising current
i_o =instantaneous core loss current
i_m = i_t with its DC component removed
i_1 = instantaneous primary side current
$i_2 + \bar{I}_2$ = instantaneous secondary side current
$\bar{I}_2$ = mean value of secondary side current
i_2 = instantaneous secondary side current with $\bar{I}_2$ removed
$i_1' = i_2$ referred to the primary side
N_1 / N_2 = primary to secondary effective turns ratio
P = permeance
F = magnetomotive force
ω = supply frequency in radians/sec
t = time

R_o = per phase core loss resistance
L_0 = zero sequence inductance = $N_1^2 P_0$
L_m = per phase magnetising reactance
L_1 = primary side per phase leakage reactance
L_2 = primary referred secondary side per phase leakage reactance
R_1 = primary side per phase winding resistance
R_2 = primary referred secondary side per phase winding resistance

I. INTRODUCTION

The question of DC injection into the AC network has received significant attention over recent years [1-15]. The DC current could be geomagnetically induced [1,2] or could be due to power electronic equipment operating under normal conditions [3,9] or under abnormal conditions [10-12]. Depending on the level and duration of DC injection, possible adverse effects that may result from it are transformer half cycle saturation, AC current distortion, transformer overheating [1,2], increased reactive power demand [13], corrosion of grounding equipment [5], metering errors and malfunctioning of protective equipment [1].

This paper focuses on the prediction of magnetising current distortion resulting from DC offset currents on the load side of single phase and three phase three limb core type transformers. Price [1] uses a time-stepping approach to analyse the effects of balanced DC injection on several types of transformers. Girgis and Ko [2] also confine their study to balanced DC injection and investigate only shell type transformers. Fuchs, You and Roesler [14] propose a model to evaluate the effects of DC bias currents on three-limb core type transformers. The electromagnetic model used here is similar to theirs. In this

paper, however, the DC bias appears explicitly on the load side of the transformer model and formed part of the load current during laboratory testing. There are also differences in the procedures used to solve the non-linear magnetic circuit equations. Fuchs and You [15] extended the model developed in reference [14] so that distortion in the primary currents due to DC bias can be evaluated under load conditions. Their model is limited to sinusoidal load currents. In this paper the load currents are assumed to be known either from calculations or from measurements and there are no restrictions on their waveshapes.

The non-linear magnetic characteristics of a transformer core are needed to predict distortion of its primary current due to DC injection. Fuchs, Masoum and Roesler [16] argue that the cross and with grain B-H curves of core lamination samples do not, by themselves, adequately represent the transformer core characteristics because of intersheet and butt-to-butt airgaps. They carry out quasi three dimensional modelling, using the finite difference method, with geometric data and material properties in the form of cross and with grain B-H curves, to deduce the core non-linear magnetic characteristics. Transformer magnetisation curves can also be obtained by measurement. A measurement technique for the three-limb core type three-phase transformer is proposed by Fuchs and You [15]. This essentially requires measurement of higher than rated applied voltages and no-load currents. The applied voltage must be high enough to saturate the core to the required level. The measurement method proposed in this paper has a significant advantage since the applied voltage does not have to exceed rated value.

II. SINGLE PHASE TRANSFORMER MODELLING

The traditional transformer equivalent circuit is essentially the representation of a real transformer as a perfect transformer to which circuit elements are connected to represent the transformer imperfections. Power losses are represented by resistances, leakage flux by leakage inductances and finite core permeability by the magnetising inductance. Figure 1 is such an equivalent circuit. The resistance and reactances making up the equivalent circuit are generally non-linear. Core loss resistance R_o, for example, depends on the frequency and waveshape of the induced voltage. Saturation may have some influence on leakage reactance [16]. The decision regarding which circuit non-linearities to ignore and which ones to consider depends on the transformer operating features that are being investigated. Here the focus is on distortion of the magnetising current. Therefore the nonlinear behaviour of L_m is considered in detail. All other non-linearities have been ignored. It is recognised that under extreme saturation, as would occur under some fault conditions [10-12], the assumptions of constant leakage inductances and constant effective turns ratio would not be valid. The detailed magnetic field analysis that would be necessary to evaluate performance under such conditions is beyond the scope of this paper.

For the single phase transformer (figure 1) at steady state, we can write:

$$N_1 i_1' = N_2 i_2 \tag{1}$$

$$i_t = i_m - N_2 \bar{I}_2 / N_1 = \psi / L_m \tag{2}$$

$$i_1 = i_m + i_1' + i_o \tag{3}$$

$$e_1 = v - i_1 R_1 - L_1 \frac{di_1}{dt} \tag{4}$$

$$\psi = \int e_1 dt' + \bar{\psi} = \tilde{\psi} + \bar{\psi} \tag{5}$$

The load current is given by $\left(i_2 + I_2'\right)$. Current i_2 contains no DC component, is periodic but may be non-sinusoidal. Current $\bar{I}_2$ is the DC component in the load current. Ampere-turn balance (equation (1)) involves only the AC component of the load current. The DC component $\bar{I}_2$ does not have any influence over the reflected load current i_1'.

The core flux linkage is $\left(\tilde{\psi} + \bar{\psi}\right)$. Flux linkage $\tilde{\psi}$ contains no DC component, is periodic but may be non-sinusoidal. As a result of the DC component in the load current, a DC component $\bar{\psi}$ exists in the core flux linkage (equation(5)).

The problem to be solved may be stated as follows: Given v, i_2, $\bar{I}_2$, the transformer core magnetisation curve and values for L_1, R_o and R_1, obtain waveforms for i_m and i_1. The magnetisation curve may not be available or even if it was it may not extend far enough into the saturation region. It is now shown that the magnetisation curve may be obtained by a simple inexpensive test. This requires a half wave rectifier and a purely resistive load connected to the secondary side of the transformer. The chosen load resistance should be low enough to allow the transformer to reach the desired depth of saturation. Current waveforms obtained from tests performed on a single-phase transformer are given in figure 2. The transformer details are given in Table 1.

A transformer magnetisation curve is traditionally expressed as a $B-H$ curve. It can also be expressed as a graph of flux linkage (ψ) against total magnetising current (i_t)[16]. The equivalence between the $B-H$ curve and the $\psi - i_t$ curve can be demonstrated by multiplying both sides of equation (2) by N_1.

It can be shown that, for the half-wave rectified load being considered, the primary side current during the negative half cycle of v, is equal to the sum of the total magnetising current and the core loss current i_o. Measured primary current with the estimated core loss current removed is shown in Figure 2. Since the hysteresis curve is approximated by a single valued magnetising curve, flux linkage ψ is equal to zero when the total magnetising current i_t is equal to zero. The time instant t_0 at which i_t is equal to zero can be identified in the measured current waveform of Figure 2. That is the instant where ψ is also equal to zero. Thus at any given instant t, greater than t_0 but less that the time at which e_1 crosses zero, the value of $i_t(t)$ can be read from Figure 2 and $\psi(t)$ can be evaluated using:

$$\psi(t) = \int_{t_0}^{t} e_1 \, dt' = \frac{N_1}{N_2} \int_0^t e_2 dt' \tag{6}$$

Note that induced voltage e_2 used for the above integration is equal to the measured secondary voltage v_2, since the secondary current is equal to zero. Figure 3 is the transformer magnetisation curve which has been constructed using the test results shown in Figure 2 and the expression given in equation (6).

Having found the core magnetisation curve, the waveforms for magnetising current i_m and primary current i_1 can be obtained by using the following iterative procedure:

(1) Discretize one period of v to define a large enough number of time instants. (If descretization is too coarse then distortion of the magnetising current will not be accurately predicted.) .

(2) Make the initial assumption that $i_m = 0$ and that $i_1 = i_1'$. Current i' is obtained by using equation (1) together with given or measured values of i_2.

(3) Use the given or measured values of v and equation (4) to determine e_1.

(4) Make an initial guess for $\bar{\psi}$.

(5) For each of the time instants generated in step 1 evaluate ψ using equation (5).

(6) For each value of ψ found in step 5, use the magnetisation curve to obtain the corresponding values of i_t.

(7) Evaluate the mean of i_t and compare it with $N_2\bar{I}_2 / N_1$. If the difference is greater than the desired tolerance, then modify $\bar{\psi}$ and return to step 5. Otherwise proceed to step (8).

(8) Obtain the waveform for i_m by subtracting the mean of i_t from i_t.

(9) Compare the newly obtained waveform for i_m with the one most recently calculated or assumed. If the difference is less than the desired tolerance then consider the problem of determination of i_m and i_1 solved. Otherwise proceed to step 10.

(10) Obtain values for i_o by using $i_o = e_1 / R_0$.

(11) Obtain the primary current waveform by using equations (3) and return to step 3.

The above steps form two iterative loops. The inner loop is for the determination of $\bar{\psi}$ and the magnetising current (i_m) waveform for a given induced voltage (e_1) waveform. The outer loop is for updating the e_1 waveform using equation (4) after each convergence of the inner loop.

III. SINGLE PHASE TESTS

The procedure detailed in section II was used to predict the magnetising and primary current waveforms under different loading conditions. The magnetising current waveform (i_m) corresponding to a DC injection ($\bar{I}_2$) of 150 mA is shown in Figure 4. It can be deduced from the waveform and equation (3) that the primary current will experience maximum distortion near the negative to positive zero crossing of the supply voltage, that is near time $t = 0$. This is confirmed by the measured current waveform of Figure 5. If there were no distortion, the zero crossing of the current waveform would occur very close to the time origin because the power factor is unity. This is also the time when the core is most saturated resulting in the transformer drawing a relatively large magnetising current which in turn causes substantial distortion of the primary current. Results of tests performed with different power factor loads were also in good agreement with theoretical predictions.

IV. THREE-LIMB TRANSFORMER MODELLING

The single phase theory presented in Section II is based on a single loop magnetic circuit whose non-linear permeance is defined by the magnetising curve of Figure 3. The same theory can be extended to model three phase transformers. The model for a 3-limb

transformer is based on the magnetic circuit shown in Figure 6. P_A, P_B and P_C represent, respectively, permeances of flux paths along the right side, centre and left side limbs of the core. P_A, P_B and P_C are non-linear because of core saturation and, generally, are not equal and are defined by different magnetisation curves. Zero sequence flux paths are represented by permeance P_o. Although a substantial proportion of the zero sequence flux path is through the transformer steel tank, the air gap between the tank and the core is sufficient for P_o to be considered constant.

The test circuit used to determine the side limb magnetising curves is shown in Figure 7. Details of the delta-star test transformer are given in Table 2. The magnetising curves were deduced in a similar way to that used to obtain Figure 3. Waveforms for i_{1A} and v_{an} were recorded and were used together with equation (7) to derive the magnetisation curve for the A-phase side limb.

$$\psi_A(t) = \frac{N_1}{N_2}\int_{t_0}^{t} v_{an}\, dt' \tag{7}$$

where t_0 is the instant of the positive to negative zero crossing of $(i_{1A} - i_{oA})$ and t is greater than t_0 but less than the time at which v_{an} crosses zero. Since the recorded waveform for i_{1C} and v_{cn} were practically identical to those of i_{1A} and v_{an}, the magnetisation curve for the C-phase side limb produced by using equation (8), is virtually identical to that of the A-phase side limb (Figure 9).

$$\psi_C(t) = \frac{N_1}{N_2}\int_{t_0}^{t} v_{cn}\, dt' \tag{8}$$

The test circuit used to determine the centre limb magnetising curve is shown in Figure 8. Waveforms for i_{1B} and v_{bn} were recorded and then used together with equation (9) to derive the magnetisation curve shown in Figure 10.

$$\psi_B(t) = \frac{N_1}{N_2}\int_{t_0}^{t} v_{bn}\, dt' \tag{9}$$

where t_0 and t are defined as was done for equation (7).

Once the three magnetising curves (Figure 9 and 10) are available, the waveforms for the magnetising currents i_{mA}, i_{mB} and i_{mC} and for primary currents i_{1A}, i_{1B} and i_{1C} (Figure 11) can be obtained by the following iterative procedure:

(1) Discretize one period of the supply voltage into small intervals in order to define a large enough number of time instants.

(2) Make the initial assumption that i_{mA}, i_{mB} and i_{mC} are equal to zero and that $i_{1A} = i_{1A}'$, $i_{1B} = i_{1B}'$ and $i_{1C} = i_{1C}'$.

(3) Use the given or measured values of v_{AB}, v_{BC} and v_{CA} and equations (10), (11) and (12) to determine the primary side induced voltages e_{AB}, e_{BC} and e_{CA}.

(4) Make an initial guess for $\bar{\psi}_A$, $\bar{\psi}_B$ and $\bar{\psi}_C$.

(5) For each of the time instants defined in step (1) evaluate ψ_A, ψ_B and ψ_C using equations (13),(14) and (15).

$$e_{AB} = v_{AB} - i_{1A}R_{1A} - L_{1A}\frac{di_{1A}}{dt} \tag{10}$$

$$e_{BC} = v_{BC} - i_{1B}R_{1B} - L_{1B}\frac{di_{1B}}{dt} \tag{11}$$

$$e_{CA} = v_{CA} - i_{1C}R_{1C} - L_{1C}\frac{di_{1C}}{dt} \tag{12}$$

$$\psi_A = \int e_{AB}\, dt' + \bar{\psi}_A = \tilde{\psi}_A + \bar{\psi}_A \tag{13}$$

$$\psi_B = \int e_{BC}\, dt' + \bar{\psi}_B = \tilde{\psi}_B + \bar{\psi}_B \tag{14}$$

$$\psi_C = \int e_{CA}\, dt' + \bar{\psi}_C = \tilde{\psi}_C + \bar{\psi}_C \tag{15}$$

(6) For each value of ψ_A, ψ_B and ψ_C found in step (5), use the magnetisation curves of Figures 9 and 10 to get the corresponding values of F_A / N_1, F_B / N_1 and F_C / N_1.

(7) For each time instant evaluate F_t / N_1, which is defined in Figure 6, using:

$$F_t / N_1 = \left(\psi_A + \psi_B + \psi_C\right) / L_o \tag{16}$$

where L_o is the zero sequence inductance.

(8) For each time instant evaluate i_{tA}, i_{tB} and i_{tC} using:

$$i_{tA} = F_A / N_1 + F_t / N_1 \tag{17}$$

$$i_{tB} = F_B / N_1 + F_t / N_1 \tag{18}$$

$$i_{tC} = F_C / N_1 + F_t / N_1 \tag{19}$$

(9) Evaluate the mean of i_{tA}, i_{tB} and i_{tC} and compare them, respectively, with $N_2\bar{I}_{2a} / N_1$, $N_2\bar{I}_{2b} / N_1$ and $N_2\bar{I}_{2c} / N_1$. If any one of the differences is greater than the desired tolerance then modify $\bar{\psi}_A$, $\bar{\psi}_B$ and $\bar{\psi}_C$ and return to step (5). Otherwise proceed to step (10).

(10) Obtain waveforms for i_{mA}, i_{mB} and i_{mC} by subtracting from i_{tA}, i_{tB} and i_{tC} their respective mean values.

(11) Compare the newly obtained waveforms for i_{mA}, i_{mB} and i_{mC} with the ones most recently calculated or assumed. If differences are less than the desired tolerance then consider the problem of determining the magnetising currents and primary currents solved. Otherwise proceed to step (12).

(12) Obtain core loss currents i_{0A}, i_{0B} and i_{0C}.

(13) Obtain the phase currents i_{1A}, i_{1B} and i_{1C} by using:

$$i_{1A} = i_{mA} + N_2 i_{2a} / N_1 + i_{oA} \tag{20}$$

$$i_{1B} = i_{mB} + N_2 i_{2b} / N_1 + i_{oB} \tag{21}$$

$$i_{1C} = i_{mC} + N_2 i_{2c} / N_1 + i_{oC} \tag{22}$$

(14) Return to step (3).

V. THREE-PHASE TESTS

The procedure detailed in Section 4 was used to predict the magnetising current and primary current waveforms under different DC injection regimes. Examples of predicted magnetising currents are shown in Figures 12 and 13. As expected magnetising current distortion is most severe near the instants when one of $|\psi_A|$, $|\psi_B|$ or $|\psi_C|$ reaches its peak value. Figures 12 and 13 show that different DC injection regimes lead to different distortion patterns. In Figure 12 distortion is centred where ψ_A reaches its negative peak since the DC component is present in A-phase only. In Figure 13, the distortion is centred where ψ_A reaches its negative peak and where ψ_C reaches its positive peak because $\bar{I}_{2a} = -\bar{I}_{2c}$. The value of the zero sequence inductance has a significant influence

on the distortion pattern. A relatively high value of L_0 has a decoupling effect on the main legs of the magnetic circuit. That is, if L_0 is large enough then DC injection in a particular phase tends to cause distortion that is restricted to that phase with the other two phases unaffected. On the other hand a reduction in L_0 causes reduced distortion of current in the phase or phases in which DC is injected and increased distortion in the other phase or phases. The fundamental reason for this is the increased influence of mmf F_t as L_0 gets smaller (equation(23)).

An example of measured primary currents is given in Figure 14. With an assumed value of 2mH for L_0, there is reasonable agreement with theoretical predictions. As expected the A-phase current is the most severely distorted around $t = 0$ whereas phase C is the one most severely affected 60^0 later. There were also good agreement between theoretical predictions and measured primary currents for other patterns of DC injection. In particular, it was confirmed by measurements that, due to the small value of L_0, the zero sequence component of DC injection causes very little distortion of the magnetising current.

VI. CONCLUSIONS

A systematic procedure has been proposed for the prediction of transformer magnetising current distortion resulting from secondary side DC currents. The procedure, which has been applied to a single phase transformer and a three-limb three-phase transformer, can be extended to the five limb three-phase transformer. A simple technique has also been proposed for the experimental determination of the transformer magnetisation

characteristics. The main advantage is that the technique does not require the supply voltage to transformer winding to be higher than the rated value. Once the magnetisation curves are available the procedure that has been presented allows prediction of primary current distortion. There are reasonable agreement between measured currents and those predicted by the proposed method. It has also been confirmed both theoretically and experimentally that in the case of the three-limb three phase transformer, provided the zero sequence inductance is low enough, only non-zero sequence DC currents cause significant core saturation and primary current distortion.

References

1. Price P R, 'Geomagnetically Induced Effects on Transformers ', IEEE Transactions on Power Delivery, vol 17, No. 4, October 2002, pp1002 – 1008
2. Girgis R S, Ko C D, ' Calculation techniques and results of effects of GIC currents as applied to two large power transformers ', IEEE Transactions on Power Delivery, vol 17, No. 2, April 1992, pp 699-705
3. Bradley S, Crabtree J, ' Effects of DC from embedded generation on residual current devices and single-phase metering ', EA Technology STP Report No. 5862, February 2000
4. University of Strathclyde, 'DC Injection into Low Voltage AC Networks ', Report on Project WS4-P11, June 2005
5. Khalid M , Ledwich G, 'Grid Connection Without Mains Frequency Transformers', Journal of Electrical and Electronic Engineering, Australia, vol 19, Nos 1 & 2, June 1999, pp 31-36
6. Collinson A, Thornycroft J, 'Low Voltage Grid Connection of Photovoltaic Power Systems ', EA Technology STP Report Number 5010, September 1999
7. Infield D G , Onions P, Simmons A D, Smith G A, 'Power Quality From Multiple Grid-Connected Single-Phase Inverters ', IEEE Transactions on Power Delivery, vol 19, No. 4, October 2004, pp 1983-1989
8. Nakajima T, Suzuki K I, Yajuna M, Kawakami N, Tanomura K I, Irokawa S, 'A new control method preventing transformer magnetization due to voltage source self-commutated converters ', IEEE Transactions on Power Delivery, vol 11, No. 3, July 1996, pp 1522-1528
9. Verhoeven B, 'Utility Aspects of Grid-Connected Photovoltaic Power Systems', International Energy Agency, Report IEA PVPS T5-01:1995, December 1998
10. Napieralska-Juszczak E, Jablonski M.,'Representation of faults in mathematical model of converter set ', Proceedings of EPE, Second European Conference on PowerElectronics and Applications, 1987,vol 2, pp. 783-788, Grenoble, France.
11. Napieralska-Juszczak E, Jablonski M.,'The FEM analysis of the non symmetrical short circuit forces and fields in the windows of convetor transformer' The International Journal for Computation and Mathematics in Electrical Engineering, vol II , No. 1, pp 213-216, COMPEL, James and James Science Publishers Ltd, London,1992

12 , Jablonski M, Napieralska-Juszczak E, 'The FEM analysis of magnetic field in convertor transformer during faults',Electromagnetic Fields in Electrical Engineering, Plenum Press, New York, pp 101-106,1988

13. You Y, Fuchs E F, Lin D, Barnes P R, 'Reactive power demand of transformers with DC bias', IEEE Industry Applications Society Magazine, Vol 2, No 4, July/August 1996, pp 45-52.
14. Fuchs E F, You Y, Roesler D J, 'Modeling and Simulation, and Their Validation of Transformers with Three Legs under DC Bias', IEEE Transactions on Power Delivery, Vol 14,No. 2, April 1999, pp 443-449.

15 Fuchs E F, You Y, 'Measurement of λ-i Characteristics of Asymmetric Three-Phase Transformers and Their Applications', IEEE Transactions on Power Delivery, Vol 17, No. 4, October 2002, pp 983-990.

16.Fuchs E F, Masoum M A S, Roesler D J, ‘Large Signal Non-Linear Model of Anisotropic Transformers for Nonsinusoidal Operation, Part I: λ-i Charateristic’, IEEE Transactions on Power Delivery, Vol 6, No 1, January 1991,pp 174-186

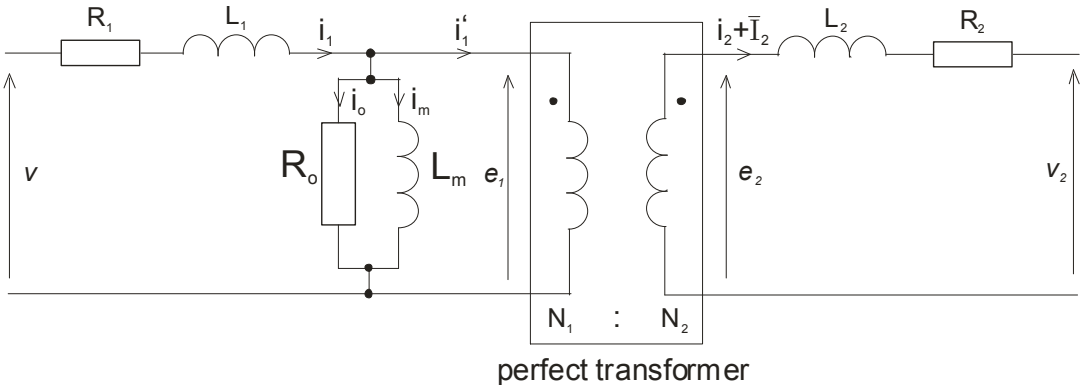

Figure 1: Single Phase Transformer Model

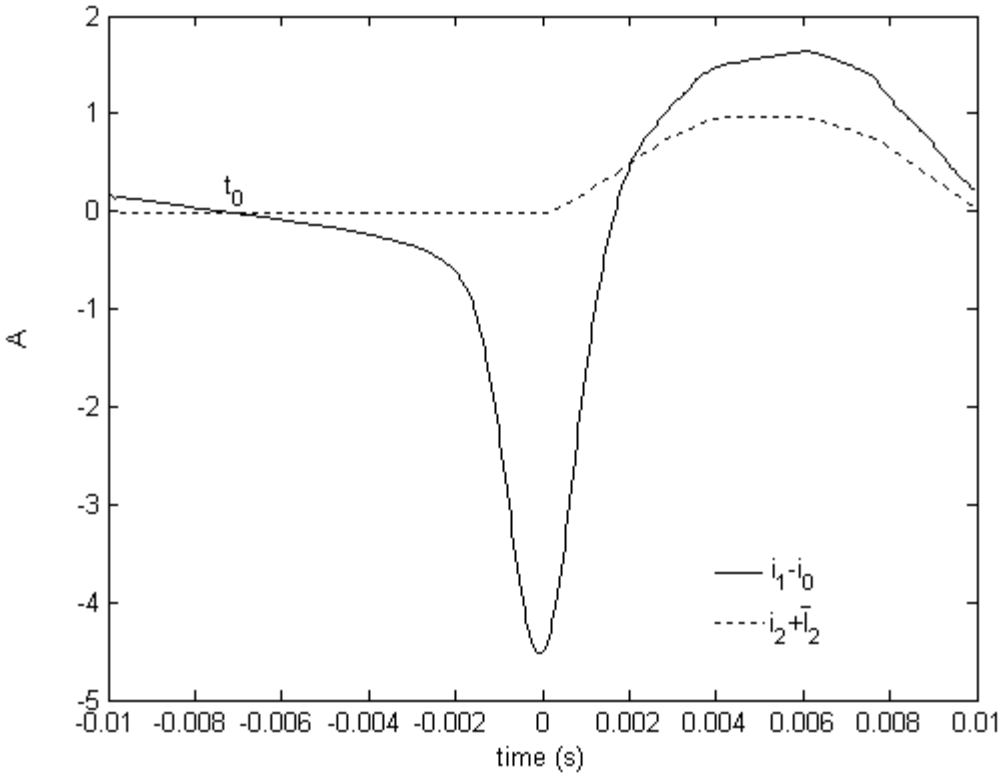

Figure 2: Measured current waveforms.
(Estimated core loss current removed)

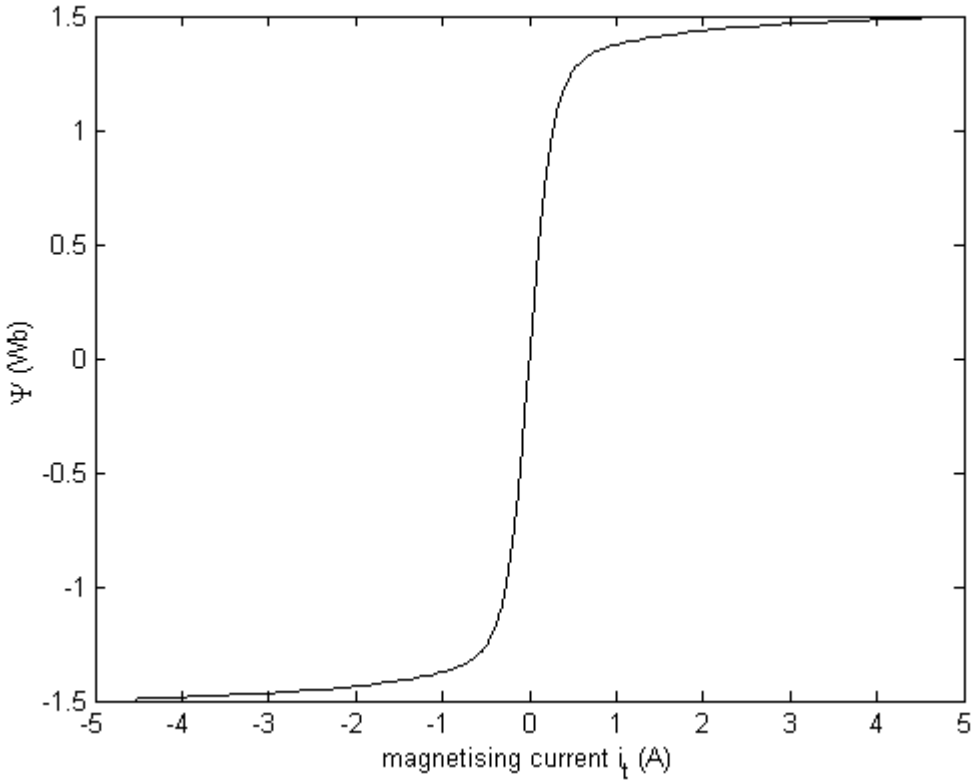

Figure 3: Magnetising curve deduced from Figure 2 and equation (6).

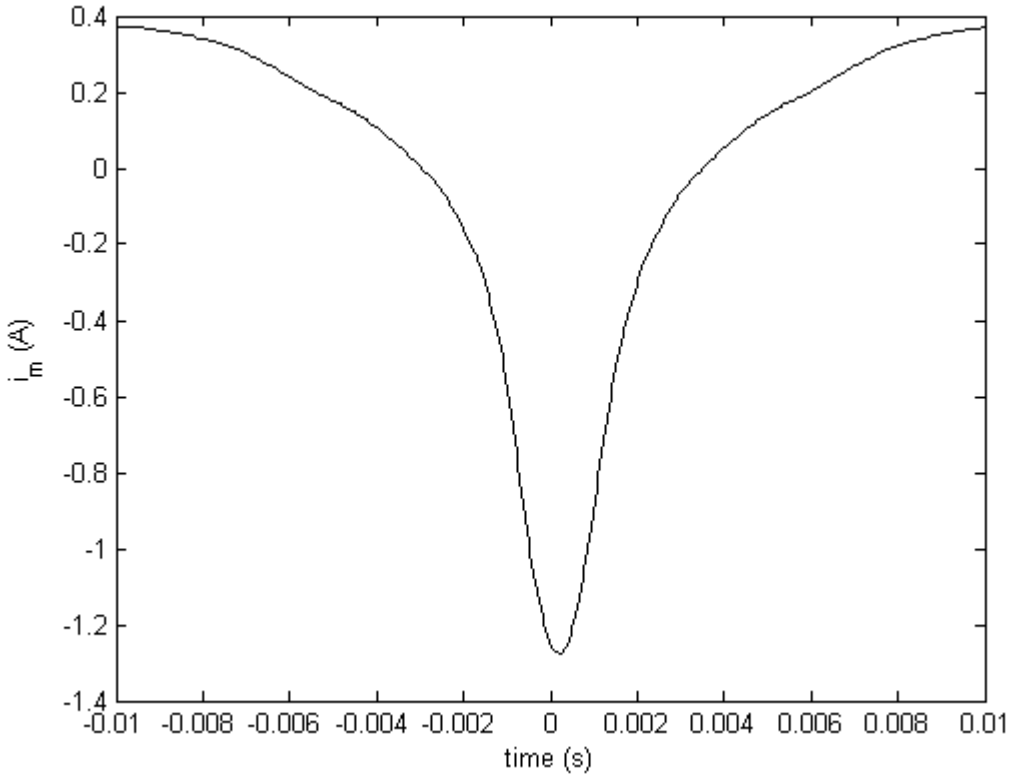

Figure 4: Predicted magnetising current distortion due to a secondary side DC current of 150mA.

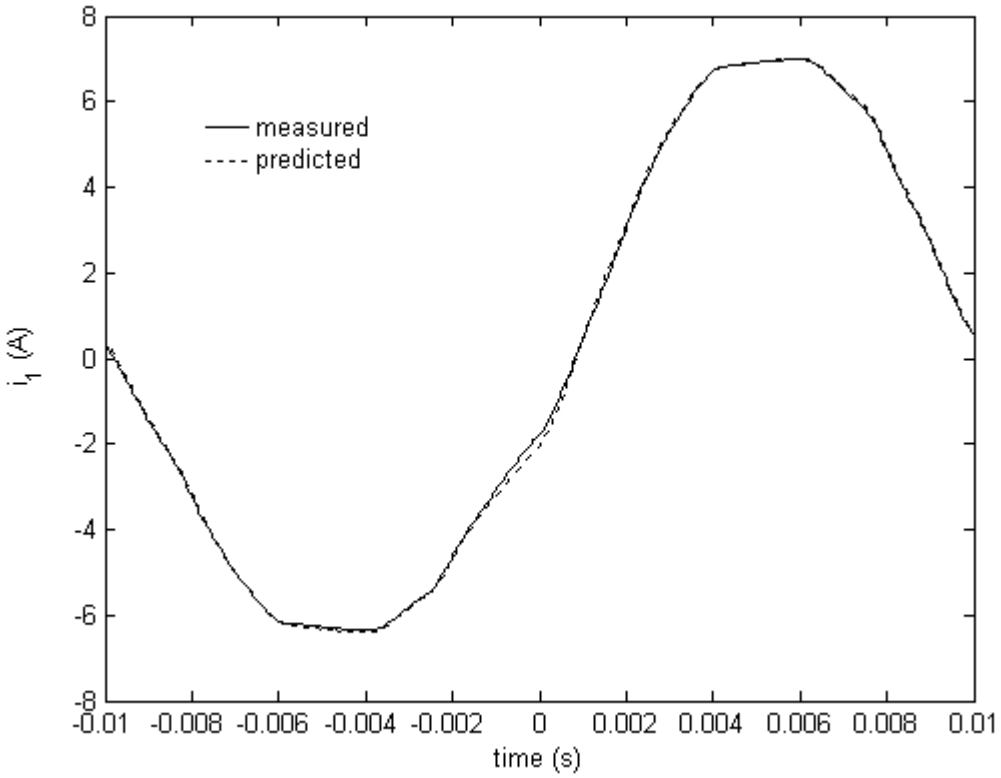

Figure 5. Primary current waveforms with unity power factor load.
(Secondary DC injection = 150 mA)

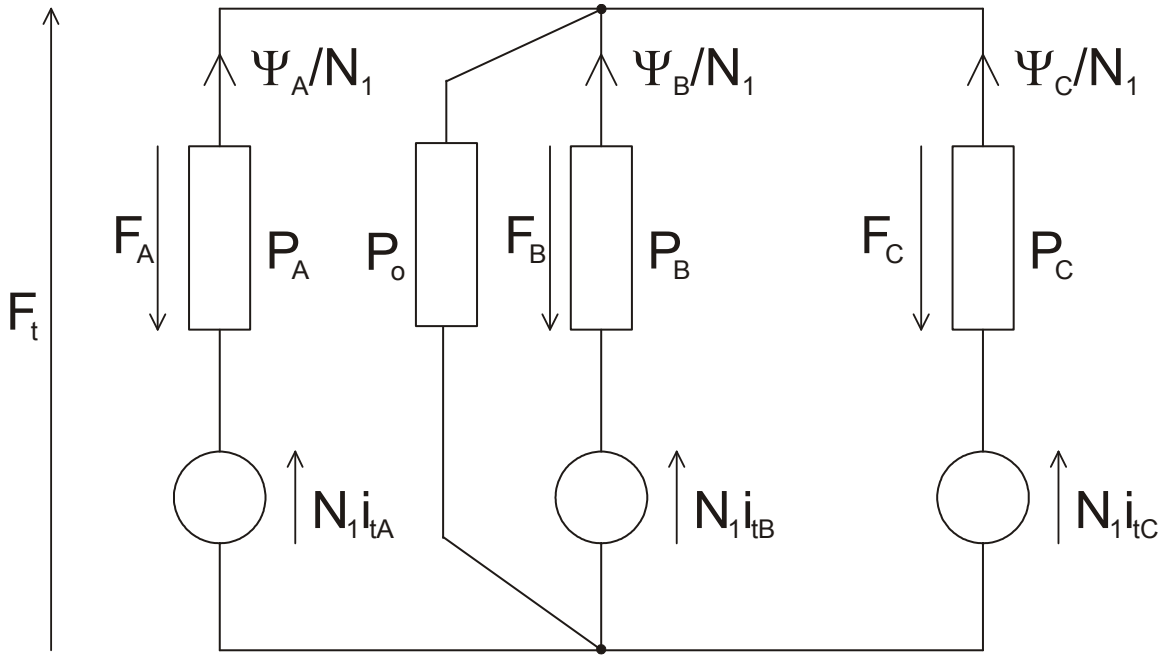

Figure 6: Magnetic circuit model of a 3-limb, 3-phase transformer

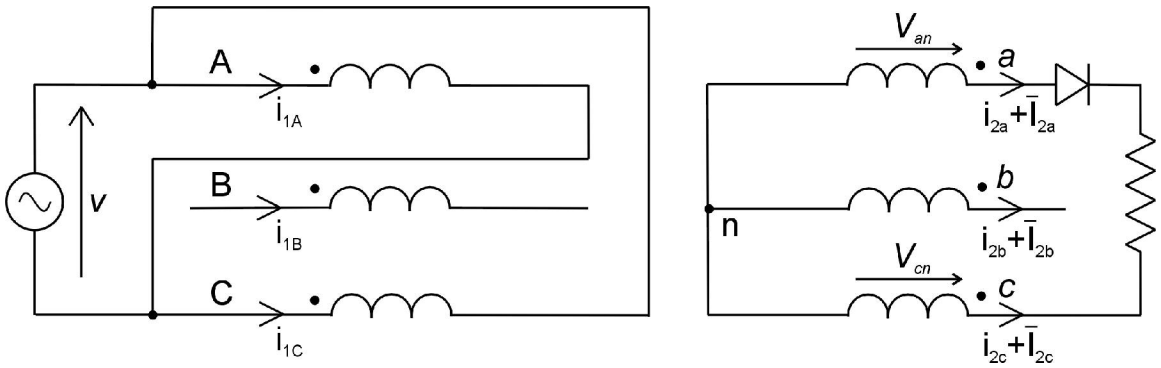

Figure 7: Test circuit to determine the side limb magnetizing curves

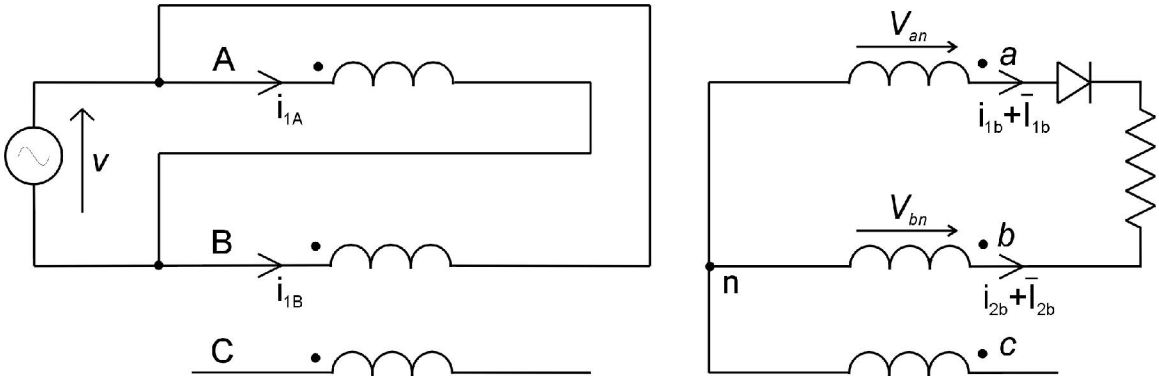

Figure 8: Tests circuit to determine the central limb magnetizing curve

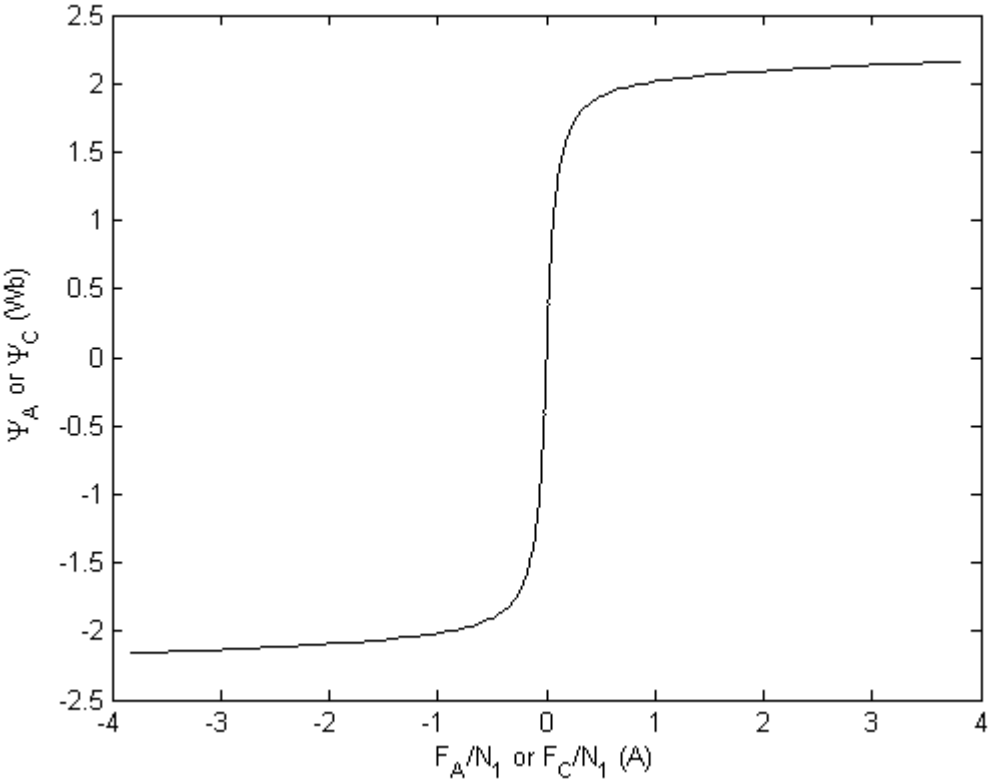

Figure 9: Side limb magnetising curve.

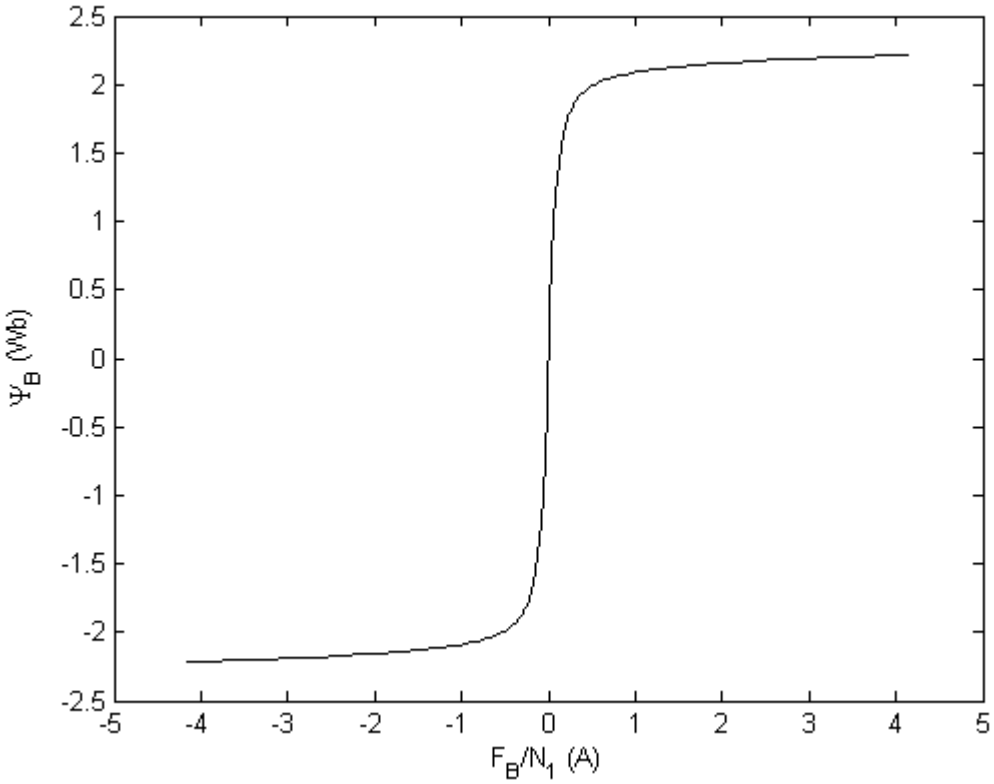

Figure 10: Centre limb magnetising curve.

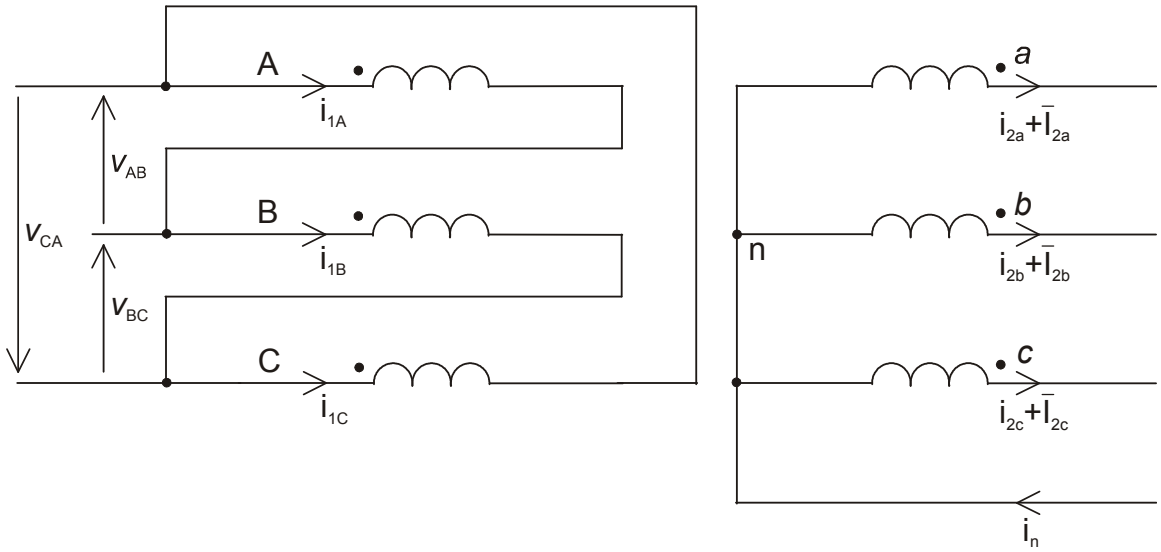

Figure 11: 3-phase transformer with DC injection.

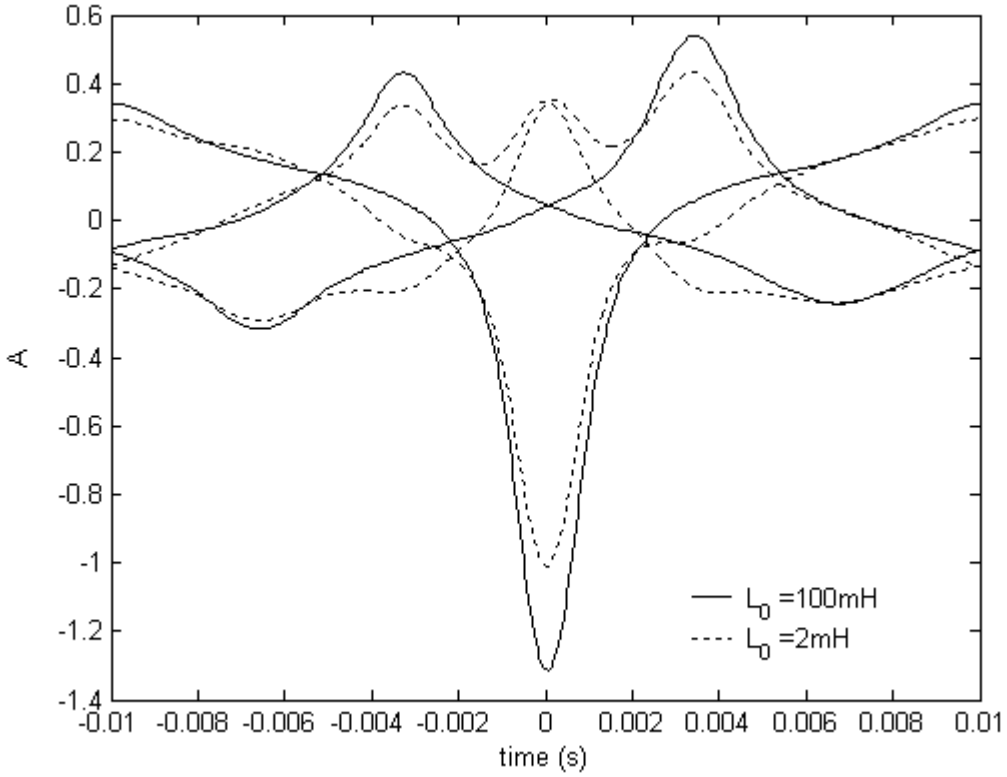

Figure 12: Predicted magnetising current with $\overline{I}_{2a} = 0.62A$, $\overline{I}_{2b} = 0A$ and $\overline{I}_{2c} = 0A$.

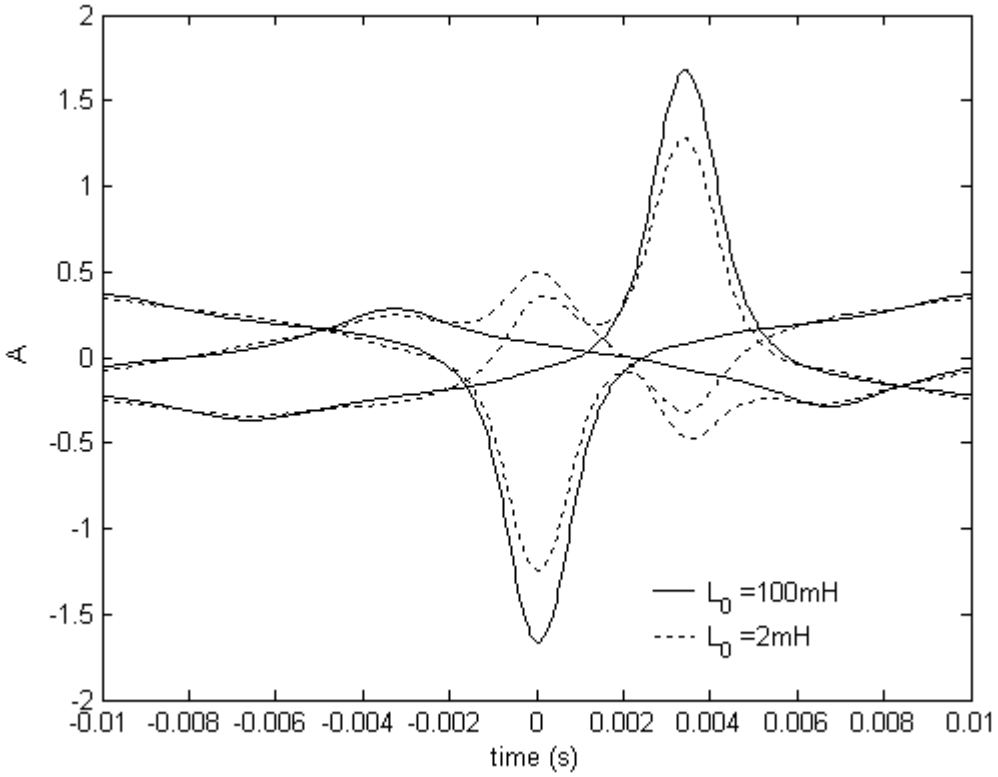

Figure 13: Predicted magnetising currents with $\overline{I}_{2a} = 0.62A$, $\overline{I}_{2b} = 0A$ and $\overline{I}_{2c} = -0.62A$.

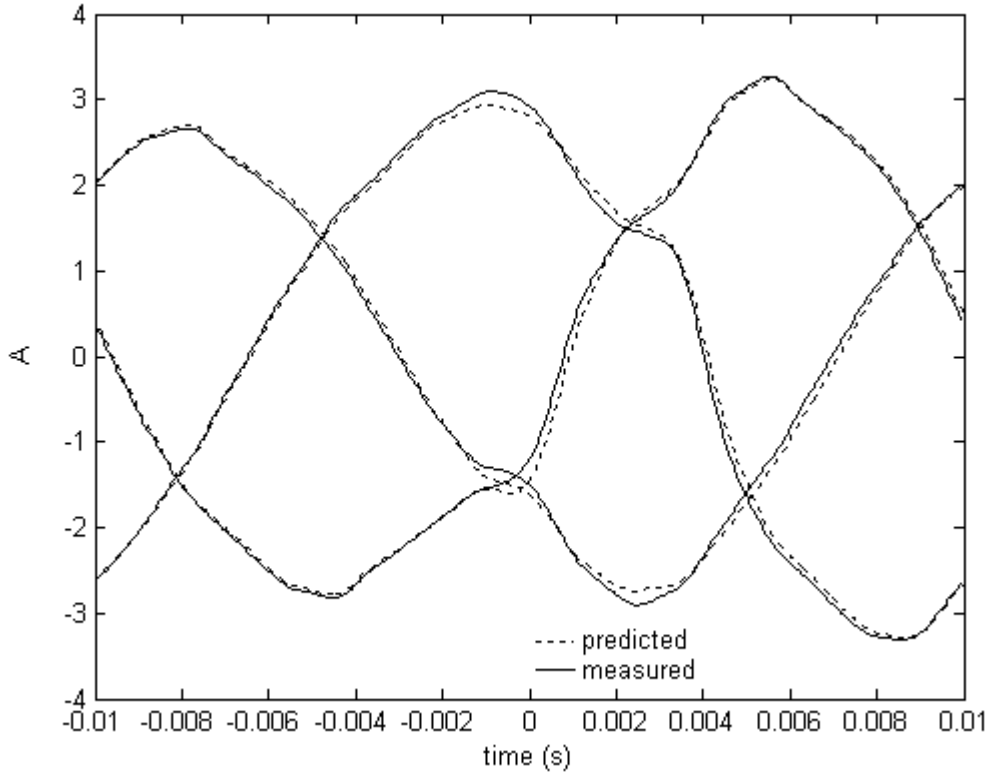

Figure 14: Comparison between predicted and measured primary currents (unity power factor load, $\overline{I}_{2a} = 0.62A$, $\overline{I}_{2b} = 0$, $\overline{I}_{2c} = -0.62A$)

Table 1: Single Phase Transformer Data

Rated Primary voltage (V)	240
Rated Secondary voltage (V)	415
Rated Primary current (A)	3
Rated Secondary current (A)	5
VA rating	1200
Rated Frequency (Hz)	50
Primary referred total leakage reactance (Ω)	1
Primary winding DC resistance (Ω)	0.65
Secondary winding DC resistance (Ω)	1.5
Coreloss resistance (Ω)	1500

Table 2: Three-Phase Transformer Data

Rated Primary voltage (V)	415
Rated Secondary voltage (V)	112/205
Rated Primary current (A)	12.8
Rated Secondary current (A)	25.4
VA rating	9176
Rated Frequency (Hz)	50
Primary per-phase DC winding resistance (Ω)	0.7
Secondary per-phase DC winding resistance (Ω)	0.5
Primary referred per-phase total leakage reactance (Ω)	1.0
Per-phase coreloss resistance (Ω)	1200